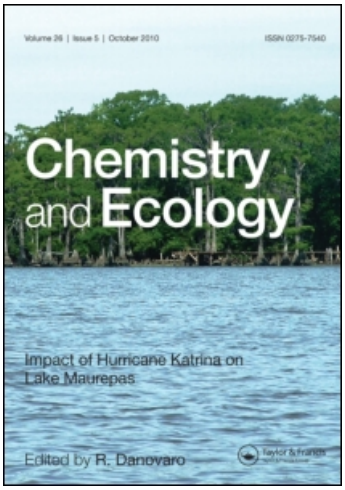

Chemistry and Ecology
Publication details, including instructions for authors and subscription information:
http://www.informaworld.com/smpp/title~content=t713455114

Humic substances as a background electrolyte in capillary electrophoresis

M. Übner[a]; M. Kaljurand[b]; M. Lopp[b]
[a] Health Resort Laboratory, Pärnu College of Tartu University, Pärnu, Estonia [b] Department of Chemistry, Tallinn University of Technology, Tallinn, Estonia

Online publication date: 30 September 2010

To cite this Article Übner, M. , Kaljurand, M. and Lopp, M.(2010) 'Humic substances as a background electrolyte in capillary electrophoresis', Chemistry and Ecology, 26: 4, 157 — 165
To link to this Article: DOI: 10.1080/02757540.2010.494157
URL: http://dx.doi.org/10.1080/02757540.2010.494157

Chemistry and Ecology
Vol. 26, Supplement, October 2010, 157–165

Taylor & Francis
Taylor & Francis Group

Humic substances as a background electrolyte in capillary electrophoresis

M. Übner[a]*, M. Kaljurand[b] and M. Lopp[b]

[a]*Health Resort Laboratory, Pärnu College of Tartu University, Pärnu, Estonia;* [b]*Department of Chemistry, Tallinn University of Technology, Tallinn, Estonia*

(*Received 15 September 2009; final version received 14 May 2010*)

Humic substances (HS) as a background electrolyte in capillary electrophoresis afford the possibility to characterise HS/reagent interactions. Thus, added $Pb(NO_3)_2$ reveals specific characteristic regions in electropherograms that correlate with the salt concentration. These regions form because of the on-capillary complexation of Pb^{2+} with HS: fulvic acid, hymatomelanic acid and humic acid. The formation of two complexes (Pb/HS fractions I and II), which have different mobility, was observed. Each of the HS fractions contains those complexes in a different ratio. Differences in the electropherograms apparently reflect structural differences in the fractions. The peak areas of both complexes have a good linear correlation with the concentration of injected Pb^{2+}.

Keywords: capillary electrophoresis; electrophoretically mediated microanalysis; fulvic acid; humic acid; hymatomelanic acid; Pb^{2+} complexes

1. Introduction

The classical definition of humic substances (HS) is based on their aqueous solubility, dividing HS into four fractions: (1) humic acid (HA; not soluble in water under acidic conditions, but becomes soluble at higher pH); (2) hymatomelanic acid (HMA; soluble in ethanol); (3) fulvic acid (FA; soluble in water at any pH); and (4) humin (not soluble in water at any pH) [1–3]. The major functional groups of HS include, among others, carboxylic, phenolic and aliphatic hydroxyl, carbonyl, amine and amide groups. Because of this polyfunctionality, HS are the most powerful chelating agents among natural organic substances [3–5]. In addition, they tend to form aggregates. The formation of aggregates is a highly metal-dependent process; it depends also on the nature and concentration of HS and the pH of the medium [6,7]. It is known that the addition of multiply charged cations to an HS solution changes the intramolecular forces that influence the HS molecules to coil with relatively hydrophobic interiors and hydrophilic surfaces [6]. Therefore, adding metals not only promotes aggregation, but also produces a more hydrophobic structure that may further enhance the tendency to flocculate [8,9]. So, HA removes bulk arsenic and heavy metals simultaneously from contaminated soils under alkaline conditions [10].

*Corresponding author. Email: monika.ubner@ut.ee

ISSN 0275-7540 print/ISSN 1029-0370 online

DOI: 10.1080/02757540.2010.494157
http://www.informaworld.com

At pH 7 more binding sites are available in HS, and the concentration of free heavy metal ions is low because they form inert complexes with HS. These metal/HS complexes are smaller than aggregated humic species at pH 5, but much larger than the free heavy metal ions [7]. For the above-mentioned reasons, the complexation of metal ions with HS is of great interest in understanding the transport and distribution of metal ions in nature [11].

However, metal binding to the HS fraction can also provide information about the structure of HS. It is suggested that two different types of binding sites for metal cations exist in HS: those associated with carboxylic groups and those associated with phenolic groups. Phenolic groups form complexes more easily with heavy metals [12]. Capillary electrophoresis (CE) enables us to separate the charged particles that exist or form in HS solution, without purifying HS through ion-exchange columns, which may change the properties of 'native' HS. With CE, the choice of separation buffer plays a substantial role in the formation of different equilibrium complexes and, therefore, the obtained signal. It is essential to consider the chelating properties of the separation buffer when interpretating the electrophoretic patterns [13]. It is known that the mobility of metal cations toward a cathode can be selectively moderated by complexation within the capillary, followed by the formation of metal complexes with different stability and effective charge [14,15]. If the pH of the medium in the capillary is around 7, the acidic carboxylic groups of HS solutes are deprotonated (negatively charged). In the case of uncoated capillaries, the presence of the negative charge allows easy separation of HS solutes by CE [16]. The wall of the capillary, negatively charged by the ionisation of silanol groups, attracts positively charged ions from the buffer, creating an electrical double layer. When a voltage is applied across the capillary, the cations of the double layer migrate to the cathode, creating a net flow of buffer solution to the negative electrode [17]. It is known that, in HS analysis using CE, sorption of HS onto the walls of uncoated silica capillaries occurs, leading to an usually long retention time and the need for high sample concentrations [16,18]. Modification of the capillary walls and the addition of other ingredients to the buffer can reduce the sorption problem. Thus, Fetch et al. [19] used magnesium (II) salt to eliminate the adsorption of HA on an uncoated capillary wall. Schmitt et al. [17] and de Moraes and Rezende [20] used ordinary buffers (acetate, phosphate, carbonate, borate) with the HA additive as a background electrolyte at different pH values to describe the affinity of several ionic pesticides [17] and naphthalene [20] for the HA. Lloyd et al. [21] used albumin at near-neutral pH, at which albumin has a negative charge and a tendency to adsorb to fused-silica capillaries. They found that this method gave better resolution for cationic analytes.

Recently, we have found that electrophoretically mediated microanalysis (EMMA) affords valuable information about the complexation of Pb^{2+} with FA [22]. To minimise HS sorption on the uncoated capillary, HS diluted solutions (natural and standard HA) were used as a background electrolyte [22,23]. Pb^{2+} represents a highly toxic compound belonging to the group of dangerous poison ions because it is cumulative in soils and natural organisms [24]. In this study, we investigated differences in the interaction of Pb^{2+} with HS fractions used as a background electrolyte, in order to characterise the binding sites of those fractions.

2. Experimental procedures

Analytical grade $Pb(NO_3)_2$ was purchased from Aldrich, NaOH from BDH (UK) and HCl from Riedel de Haën (Germany). HS were extracted from Baltic Sea sediment (Haapsalu Bay, northwest of Estonia). The experimental procedure of separating HS fractions has been described previously by Übner et al. [25]. In this study, non-lyophilised HS were used to avoid changes in their molecular structure. A stock solution of HA (4.8 mg·mL^{-1}) was prepared by weighing a given

amount of corresponding gel and diluting it to a fixed volume using Milli-Q water (Millipore). Stock solutions, HA gel, HMA (2.5 mg·mL^{-1}) and FA (6.2 mg·mL^{-1}) solutions were stored at 4 °C. HS fractions were employed separately as a background electrolyte component. HA, HMA and FA solutions were prepared daily by dissolving the appropriate amount of initial stock solution (depending on their concentration) in Milli-Q water. The electrolyte was filtered through a Millipore 0.45 μm membrane filter. The concentration of each HS fraction in the background electrolyte was 0.1 mg·mL^{-1}, and the pH was adjusted to 7 with 0.2 M NaOH solution (Na-salt form). The standard metal ion solution was diluted from the 0.01 M $Pb(NO_3)_2$ stock solution using Milli-Q water. Pb^{2+} solutions were prepared in the range 1×10^{-4} to 6×10^{-4} M.

All CE experiments were performed with an ISCO CV^4 capillary electropherograph model 3850, which was thermostated with forced air using a fan. The bare fused-silica capillary 75 μm i.d. (Polymicro Technologies, Phoenix, AZ, USA) had a total length of 80 cm (48 cm to the detector). The UV absorbance signal of the solution was recorded at 226 nm. Experiments were performed at room temperature. The equipment and procedures used were described in our previous work [22,26]. A plug of metal salt solution was injected hydrodynamically (for 15 s) into the capillary filled with HA, HMA or FA as the electrolyte, and after injection, a high voltage (20 kV) was applied. Upon application of an electric field, the zone of injected Pb^{2+} cations merges with the HS because of differences in their electrophoretic mobilities. The positively charged Pb^{2+} ions and HS anions mix and form different complexes. The resultant products in equilibrium migrate from the reaction zone (injection zone) and separate because the electrophoretic mobilities of the products differ from those of the HS anions. During all experiments, current values were in the range 1–3 μA. The electro-osmotic flow (EOF) velocity was estimated by using nitromethane as a marker compound each day. The calculated EOF mobility values were: $(8.5 \pm 0.2) \times 10^{-4}$ cm^2·V^{-1}·s^{-1} for FA; $(8.5 \pm 0.1) \times 10^{-4}$ cm^2·V^{-1}·s^{-1} for HA; and $(8.1 \pm 0.4) \times 10^{-4}$ cm^2·V^{-1}·s^{-1} for HMA. All experiments were performed in triplicate.

3. Results and discussion

3.1. *Electropherograms of HS fractions*

When HS fractions are used as the background electrolyte without adding a metal salt, a steady baseline is obtained. We have previously found that after injecting a Pb^{2+} plug into FA solution, three main characteristic regions form in the electropherogram [22]. Here, we found that the other water-soluble HS fractions (HMA and HA), if used as a background electrolyte together with a Pb^{2+} solution, form reproducible electropherograms that are similar to, but characteristic of, each HS fraction. The typical electropherograms recorded after injection of 6×10^{-4} M $Pb(NO_3)_2$ solution into different background electrolytes are shown in Figure 1. All electropherograms can be divided into three regions: (1) a positive relatively symmetrical sharp peak, (2) a broad negative peak, and (3) a wide triangular peak with a plateau at the end.

Because we also observed that HS without metal ions gave electropherograms with a straight baseline only, the formation of characteristic new peaks strongly suggests that these were evoked by an interaction between the metal ions and HS. It may be suggested that two humps in the electropherograms, regions 1 and 3, indicate the formation of at least two different types of Pb^{2+} and HS complexes. These complexes should have an overall negative charge (the HS at the pH 7 used in background electrolytes have in total a negative charge) and are carried towards the cathode only because of the stronger EOF flow. The negative area of region 2 should express an absence of charged particles, which is formed by removing HS anions from the reaction zone in both directions – towards regions 1 and 3. The main EOF flow of the buffer carries complexes and the vacancy zone towards the cathode.

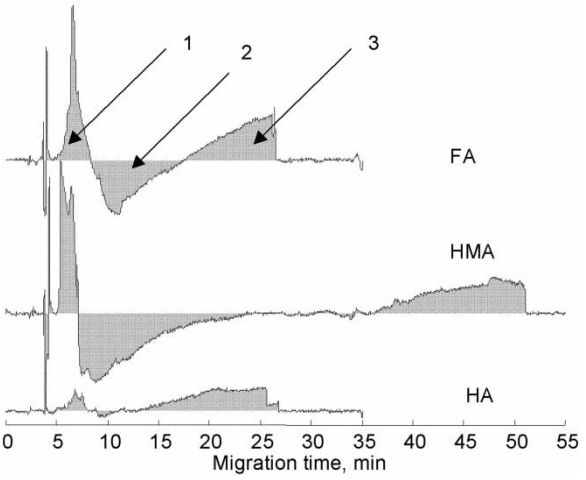

Figure 1. Electropherograms of Pb^{2+} solution when HA, HMA and FA were used as background electrolytes. Separation voltage, 20 kV; hydrodynamic injection of 6×10^{-4} M $Pb(NO_3)_2$, 15 s; pH 7; detection at 226 nm; fused-silica capillary 80 cm × 75 μm.

Table 1. The correlation of peak areas of regions 1, 2 and 3 with the concentration of the added $Pb(NO_3)_2$.

		$\times 10^5$ area[a]				Linear regression	
Region	HS fraction	Pb^{2+} 1×10^{-4} M	Pb^{2+} 2×10^{-4} M	Pb^{2+} 4×10^{-4} M	Pb^{2+} 6×10^{-4} M	R^2	Slope[b]
1	HA	1.2 ± 0.1	1.5 ± 0.2	3.0 ± 0.5	4.5 ± 0.1	0.9823	0.7628
	HMA	2.5 ± 0.2	7.8 ± 1.0	22.5 ± 4.3	35.4 ± 1.9	0.9731	5.6239
	FA	3.5 ± 0.4	5.4 ± 0.6	23.2 ± 1.1	26.3 ± 3.1	0.9313	4.6463
2	HA	-0.18 ± 0.03	-0.60 ± 0.06	-0.73 ± 0.13	-0.63 ± 0.11	0.5648	−0.1418
	HMA	-3.2 ± 0.2	-7.7 ± 1.1	-23.8 ± 4.0	-40.0 ± 5.7	0.9647	−6.2086
	FA	-4.3 ± 0.6	-10.7 ± 1.3	-30.7 ± 1.8	-35.7 ± 3.3	0.9588	−6.3625
3	HA	5.4 ± 0.5	11.5 ± 1.0	26.8 ± 4.7	38.7 ± 1.8	0.996	6.4526
	HMA	5.4 ± 0.4	12.7 ± 1.1	55.7 ± 9.1	68.4 ± 4.6	0.9398	11.6490
	FA	7.0 ± 0.8	14.4 ± 1.4	32.0 ± 2.0	39.3 ± 2.5	0.9788	7.0109

Notes: [a]Area values, mean ± SD, in arbitrary units. [b]Slope from the linear formula $y = ax$.

3.2. *Quantitative relationships of peak areas with added cation concentration*

One can assume that if the area of the specified region is quantitatively related to the concentration of the added metal, it should reflect the formation of the corresponding metal/HS complexes. Therefore, the peak area of regions 1, 2, and 3 is correlated with the concentration of added Pb^{2+} ions. The obtained results are presented in Table 1.

Region 1, which appears at the beginning in the electropherogram, is associated with a complex migrating by EOF towards the cathode (initially moving slowly towards the anode against EOF). For that region, a satisfactory linear correlation of peak area with Pb^{2+} concentration was obtained for all HS fractions (HA, HMA and FA; $R^2 = 0.9823$, 0.9731 and 0.9313, respectively). The obtained correlation suggests that all HS fractions form a similar metal/HS complex (Pb/HS fraction I). As expected for HS, the hump in region 1 is composed of several strongly overlapping peaks (Figure 1). These peaks may indicate the occurrence of several similar complexes, which have similar velocity in the capillary. In the case of HMA and FA, the slope of the linear correlation (Table 1) is several times greater than for HA. This observation may be connected to absorption

differences in the complexes formed in the electric field. The largest peak area was observed for HMA and the smallest for HA. This means that, in addition to absorption differences, the concentration of Pb/HS fractions I in the capillary is also significant.

Region 3 characterises the migration of apparently the slowest migrating particles (moving more quickly towards the anode and slightly slower than EOF towards the cathode). HA and FA showed an excellent linear correlation with the concentration of injected metal ($R^2 = 0.996$ and $R^2 = 0.9788$, respectively). This indicates that a second type of metal ion/HS complex (Pb/HS fraction II) may exist. The HMA also reveals the existence of that complex; however, the correlation coefficient for the peak area with the inserted metal was somewhat lower ($R^2 = 0.9398$). The largest area values for Pb/HS fraction II were found for HMA, whereas HA and FA had almost identical values. Thus, HA and FA may have almost the same amount of those functional groups that are related to the formation of Pb/HS fractions II.

Region 3, in Figure 1, is almost triangular in shape, and approaches a constant level at higher metal concentrations. The appearance of this hump may be explained as follows: if we assume that the equilibrium is substantially shifted towards the formation of Pb/HS fraction II, then a quantity of metal will be consumed by an irreversible process during migration of the sample plug along the capillary. Immediately after applying the high voltage, the number of available complexation sites on HS aggregates is limited (compared with the amount of metal ions), and the complex-forming process has zero order, resulting in the constant concentration of the Pb/HS fraction II along the capillary. If a sufficient quantity of the sample has been consumed, the process becomes the first-order formation of Pb/HS fraction II, with a decreasing concentration along the capillary. The negatively charged particles move in the opposite direction relative to the EOF, as speculated above. Pb/HS fraction II moves opposite to the EOF more quickly than the Pb/HS fraction I and, as a result, appears in the electropherograms later than Pb/HS fraction I. Thus, the resulting shape of region 3 reflects the change in concentration over time at the detector window; the lowest concentration is seen first. Further, the concentration increases until saturation is reached (change in the shape of the triangle).

It is known that HS form inner and outer sphere complexes. Outer sphere complexes form more quickly than inner sphere complexes. Outer sphere complexes may reflect the metal/HS complexes from region 1. Inner sphere complexes may be more hydrophobic. Pb^{2+}, a large and highly polarisable metal cation, might prefer ligands that are more polarisable (e.g. S-, N- and P-containing ligands) [27,28]. Therefore, Pb/HS fractions II may reflect inner sphere metal/HS complexes.

If regions 1 and 3 form HS metal complexes, the sum of the areas must correlate linearly with the Pb^{2+} concentration. Indeed, the sum of areas for regions 1 and 3 of each HS fraction has slightly better linear correlation with the injected Pb^{2+} concentration than the areas alone (Figure 2).

As shown in Figure 2, each HS fraction has a different content of both metal/HS complexes. HMA has a higher content of both complexes than HA. Differences in the complexes must reflect the content of the corresponding functional groups in the HS fraction. As can be seen from all HS fractions, Pb^{2+} gives more complexes with HMA. Evidently, that fraction has more functional groups that are suitable for Pb^{2+} complexation. Estimating from the slope value, HMA may have $\sim$1.5 times more of both complexes than FA, and 2.4 times more than HA. This is in accordance with the findings Quan and Yan [29]: that HA form more stable complexes with Pb^{2+} than FA. In our case, the HMA fraction is part of the HA fraction that is removed by ethanol and the Pb/HMA fraction is the highest.

Region 2 expresses a range of negative optical density compared with the HS-buffer solution. The negative area of region 2 should express migration of the vacancy zone of charged particles in the HS buffer, i.e. the absence of HS particles that are consumed during the formation of Pb/HS fractions I and II. The vacancy zone should migrate at the speed of the free HS anion. However, it is difficult to determine how regions 1 and 3 are related to region 2. Linear correlation of the

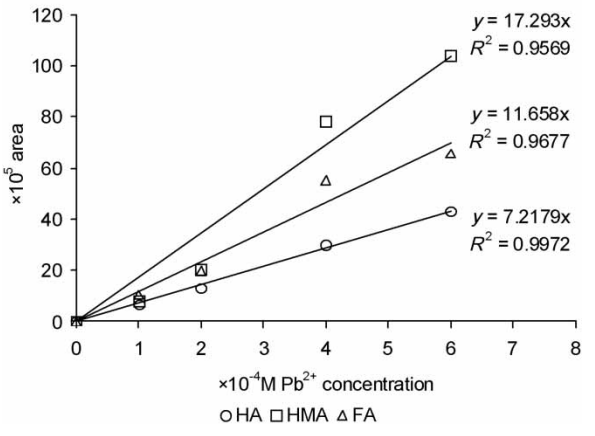

Figure 2. Dependence of the sum of areas of regions 1 and 3 on the injected Pb^{2+} concentration.

area of region 2 with the injected Pb^{2+} concentration is worse than for the other regions. The best linear correlations of the areas from the metal concentration were for HMA and FA fractions ($R^2 = 0.9647$ and $R^2 = 0.9588$, respectively). HMA had the highest vacancy area values, which are apparently related to the highest values in regions 1 and 3. Taking into account the nature of the formation of region 2, one may conclude that region 2 is not suitable for the quantitative estimation of the concentration of metal/HS complexes.

3.3. *Comparison of Pb/HS fractions I and II*

Cation binding to HS is assumed to occur through specific interactions between cations and surface functional groups and by non-specific binding to any residual negative charge. Lead is bound by HS predominantly as monodentate complexes [30]. From the literature data, it is known that Pb^{2+} forms complexes with HS via two different types of binding sites: (1) major sites, carbonyl and hydroxyl functional groups; and (2) minor sites, S-, N- and P-containing groups. Other authors have suggested the formation of two types of complexes [27,28,31]. However, according to the general understanding of the EMMA process in a capillary, the symmetrical hump corresponds to the reversible (A $\leftrightarrow$ B type) process, whereas the irreversible (A $\rightarrow$ B type) process results in the triangular hump. As explained above, the latter case may be due to continuous consumption of the reactant during its migration along the capillary and the decrease in the formation of the product, respectively (which manifests itself as a triangle on the electropherogram). Those considerations allow speculations about the possible nature of the complexes.

Reactions of HS with metal ions occur in two ways: as a major reaction, in which both carboxyl and phenolic hydroxyl groups participate simultaneously; and as a minor reaction, which involves carboxyl groups only [32]. As the metal concentration is increased, the strong binding sites become saturated and the excess metal then binds to the weaker sites, forming labile weak complexes [31]. At pH 5 and higher metal concentrations, more weak binding sites (e.g. hydroxyl or thiol groups) are occupied. These complexes move faster. Stronger binding sites for HS, such as carboxyl groups, give complexes that move slower with EOF [33]. At pH 7, carboxylic and phenolic binding sites on HS may occur, and metal binding will depend on the total HS concentration. Weak binding sites determine the behaviour of humic complexation at high metal loading, whereas strong binding sites determine the complexation strength of HS at trace metal concentrations. Moreover, phenolic sites are predominant binding sites at alkaline pH. At low HS concentrations, metal binding occurs mainly at weak sites (i.e. ~80% attribute to carboxylic groups), followed by binding at strong

sites (i.e. ∼20% attributed to phenolic moieties) [34]. In our case, region 1 may express the Pb^{2+} complexation with carbonyl and hydroxyl groups (Pb/HS fraction I). Region 3 may express the metal complexation with more hydrophobic and polarisable structures, giving Pb/HS fraction II. As shown in Table 1, region 3 (Pb/HS fraction II) always has higher area values than region 1 (Pb/HS fraction I).

When calculating the ratio of the areas for regions 3 and 1 (Table 2), we found that for all HS fractions, the ratio does not depend on the Pb^{2+} concentration. However, each fraction has its own average value for the ratio. It may be suggested that in HMA and FA the amount of Pb/HS fraction II is about two times higher than that of Pb/HS fraction I. At the same time, the relative amount of Pb/HS fraction II in HA is ∼7.3 times higher than that of Pb/HS fraction I. It may hint that in HA there are relatively more polarisable functional groups than in FA and HMA.

Of all HS fractions, HA had the highest molecular mass [2,3]. Our previous data showed that HA had a more aliphatic structure than other HS fractions [25]. The formation of inner sphere complexes may force the long carbon chains to turn outside, thus making the Pb^{2+}/HA complex more hydrophobic. HA has fewer carboxylic structures than other HS fractions (Table 1), whereas HMA and FA have twice as many hydrophobic and polarisable structures.

Comparing the elementary composition of HS fractions (Table 3, calculated from [25]) with the findings from electropherograms (Table 1), we may conclude that the amount of Pb/HS fraction I is related to the oxygen content (connected mainly with the content of carboxyl and hydroxyl groups). Also, the relative amount of Pb/HS fraction II, which decreases in the order HMA > FA > HA, is in good correlation with the calculated aromaticity values for those fractions (Table 3). Formation of Pb/HS fraction II may also be connected with different binding sites that arise from groups other than carboxyl (nitrogen-, sulphur- and oxygen-containing functional groups).

Beck et al. [35] fractionated Pb–humate complexes using free-flow electrophoresis and found that all HA constituents are able to coordinate Pb cations. Complexation causes a stronger differentiation of the electrophoretic mobility of HA constituents. At pH 6, virtually only carboxyl groups are responsible for complexation. Despite their strong complexation, HA constituents may still possess a high anionic charge. These may be pseudomicelles with a high external charge and charge centres turned towards the interior of the agglomerate. Šenkýr et al. [24] found, using stripping voltammetry, that possible fragments of HA which form complexes with Pb^{2+} are oxalic, citric and *d*-tartaric acid.

Table 2. Dependence of the ratio of areas from regions 3 and 1 on the concentration of inserted Pb^{2+} ions.

	Pb^{2+} concentration				
		$\times 10^{-4}$ M			
Region 3/Region 1	1	2	4	6	Mean ± SD
HA	4.4	7.5	8.8	8.6	7.3 ± 2.0
HMA	2.1	1.3	2.5	1.9	1.9 ± 0.5
FA	2.0	2.7	1.4	1.5	1.9 ± 0.6

Table 3. Elementary composition and aromaticity of HS fractions.

		In HS fraction, %				
Humic substances	Ash, %	C	H	N	O	Aromaticity, %
HA	33.0	33.7	5.0	4.8	23.4	13
HMA	11.8	47.6	6.0	2.6	32.0	35
FA	16.6	36.5	4.8	6.4	35.6	20

4. Conclusions

The use of HS as a background electrolyte in CE offers the possibility to follow the on-capillary chemical reactions of metal ions and HS inside the capillary (the EMMA approach). A steady HS concentration in the capillary suppresses interactions between the formed complexes and the capillary walls. The method enables one to characterise and compare different HS fractions and study their interactions with different agents. From the obtained electropherograms, we may conclude that the Pb^{2+} cation injected into the capillary with HS as a background electrolyte is related to the formation with HS of at least two different complexes (Pb/HS fractions I and II). In all HS fractions, the sum of areas of the two main positive signals shows good linear correlation with the concentration of injected Pb^{2+}. We can assume that in all HS fractions the Pb/HS fraction II prevails; however, the ratio of Pb/HS fraction II to Pb/HS fraction I is highest ($\sim$7) in HA.

Acknowledgements

We thank the Estonian Ministry of Education and Research for financial support (Doctorate Grant No. 0172062s01) and Kati Helmja for technical assistance.

References

[1] M.H.B. Hayes, *Humic substances: progress towards more realistic concepts of structures*, in *Humic Substances: Structures, Properties and Uses*, G. Davis and E.A. Ghabbour, eds., The Royal Society of Chemistry, Cambridge, 1998, pp. 1–28.
[2] D.S. Orlov, *Soil Humic Acids and General Humification Theory*, Moscow State University Publisher, Moscow, 1990 (in Russian).
[3] F.J. Stevenson, *Humus Chemistry: Genesis, Composition, Reactions*, 2nd ed., Wiley, New York, 1994.
[4] M.L. Pacheco, E.M. Peña-Méndez, and J. Havel, *Supramolecular interactions of humic acids with organic and inorganic xenobiotics studied by capillary electrophoresis*, Chemosphere 51 (2003), pp. 95–108.
[5] R.L. Cook and C.H. Langford, *A biogeopolymeric view of humic substances with application to paramagnetic metal effects on ^{13}C NMR*, in *Understanding Humic Substances: Advanced Methods, Properties and Applications*, E.A. Ghabbour and G. Davies, eds., The Royal Society of Chemistry, Cambridge, 1999, pp. 31–48.
[6] R. von Wandruszka, C. Ragle, and R. Engebretson, *The role of selected cations in the formation of pseudomicelles in aqueous humic acid*, Talanta 44 (1997), pp. 805–809.
[7] P. Chakraborty, *Study of cadmium–humic interactions and determination of stability constants of cadmium–humate complexes from their diffusion coefficients obtained by scanned stripping voltammetry and dynamic light scattering techniques*, Anal. Chim. Acta 659 (2010), pp. 137–143.
[8] P. Schmitt, A. Kettrup, D. Freitag, and A.W. Garrison, *Flocculation of humic substances with metal ions as followed by capillary zone electrophoresis*, Fresenius J. Anal. Chem. 354 (1996), pp. 915–920.
[9] N.D. Bryan, M.N. Jones, J. Birkett, and F.R. Livens, *Aggregation of humic substances by metal ions measured by ultracentrifugation*, Anal. Chim. Acta 437 (2001), pp. 291–308.
[10] S. Wang and C.N. Mulligan, *Enhanced mobilization of arsenic and heavy metals from mine tailings by humic acid*, Chemosphere 74 (2009), pp. 274–279.
[11] M. Nordén and E. Dabek-Zlotorzynska, *Study of metal–fulvic acid interactions by capillary electrophoresis*, J. Chromatogr. A 739 (1996), pp. 421–429.
[12] C. Guéguen, B. Koukal, J. Dominik, and M. Pardos, *Competition between alga* (Pseudokirchneriella subcapitata), *humic substances and EDTA for Cd and Zn control in the algal assay procedure (AAP) medium*, Chemosphere 53 (2003), pp. 927–934.
[13] S.L. de Moraes and M.O.O. Rezende, *Capillary electrophoresis (CE): a powerful tool to characterize humic acid (HA)*, J. Braz. Chem. Soc. 19 (2008), pp. 24–28.
[14] E. Naujalis and A. Padarauskas, *Development of capillary electrophoresis for the determination of metal ions using mixed partial and complete complexation techniques*, J. Chromatogr. A 977 (2002), pp. 135–142.
[15] Z.-L. Chen and R. Naidu, *On-column complexation of metal ions using 2,6-pyridinedicarboxylic acid and separation of their anionic complexes by capillary electrophoresis with direct UV detection*, J. Chromatogr. A 966 (2002), pp. 245–251.
[16] J. Peuravuori, V. Lepane, T. Lehtonen, and K. Pihlaja, *Comparative study for separation of aquatic humic substances by capillary zone electrophoresis using uncoated, polymer coated and gel-filled capillaries*, J. Chromatogr. A 1023 (2004), pp. 129–142.

[17] Ph. Schmitt, D. Freitag, I. Trapp, A.W. Garrison, M. Schiavon, and A. Kettrup, *Binding of s-triazines to dissolved humic substances: electrophoretic approaches using affinity capillary electrophoresis (ACE) and micellar electrokinetic chromatography (MEKC)*, Chemosphere 35 (1997), pp. 55–75.
[18] S. Pompe, K.-H. Heise, and H. Nitsche, *Capillary electrophoresis for a 'fingerprint' characterization of fulvic and humic acids*, J. Chromatogr. A 723 (1996), pp. 215–218.
[19] D. Fetsch, M. Fetsch, E.M. Peña-Méndez, and J. Havel, *Humic acid capillary zone electrophoresis adsorption on capillary walls, separation in metal ion supplemented buffer and the fingerprints*, Electrophoresis 19 (1998), pp. 2465–2473.
[20] S.L. de Moraes and M.O.O. Rezende, *Behaviour of humic acid as a micellar phase in micellar electrokinetic chromatography (MEKC)*, Microchim. Acta 151 (2005), pp. 115–122.
[21] D.K. Lloyd, A.-F. Aubry, and E. De Lorenzi, *Selectivity in capillary electrophoresis: the use of proteins*, J. Chromatogr. A 792 (1997), pp. 349–369.
[22] M. Übner, M. Kaljurand, and M. Lopp, *Interactions of Pb^{2+} with fulvic acid by electrophoretically mediated on-capillary microanalysis*, J. Chromatogr. A 1057 (2004), pp. 253–256.
[23] M. Übner, M. Kaljurand, and M. Lopp, *Suppression of solute–wall interactions in humic acid capillary electrophoretic analysis by its diluted solution as background electrolyte*, Colloid Surface A 302 (2007), pp. 634–637.
[24] J. Šenkýr, A. Ročáková, D. Fetsch, and J. Havel, *The acidobasic and complexation propeties of humic acids*, Toxicol. Environ. Chem. 68 (1999), pp. 377–391.
[25] M. Übner, M. Treuman, A. Viitak, and M. Lopp, *Properties of humic substances from the Baltic Sea and Lake Ermistu mud*, J. Soils Sediments 4 (2004), pp. 24–29.
[26] M. Übner, V. Lepane, M. Lopp, and M. Kaljurand, *Electrophoretic aggregation of humic acid*, J. Chromatogr. A 1045 (2004), pp. 253–258.
[27] E.M. Logan, I.D. Pulford, G.T. Cook, and A.B. Mackenzie, *Complexation of Cu^{2+} and Pb^{2+} by peat and humic acid*, Eur. J. Soil Sci. 48 (1997), pp. 685–696.
[28] K. Xia, W. Bleam, and P.A. Helmke, *Studies of the nature of Cu^{2+} and Pb^{2+} binding sites in soil humic substances using X-ray absorption spectroscopy*, Geochim. Cosmochim. Acta 61 (1997), pp. 2211–2221.
[29] G. Quan and J. Yan, *Binding constants of lead by humic and fulvic acids studied by anodic stripping square wave voltammetry*, Russ. J. Electrochem. 46, (2010), pp. 90–94.
[30] D. Gondar, R. Lopez, S. Fiol, J.M. Antelo, and F. Arce, *Cadmium, lead, and copper binding to humic acid and fulvic acid extracted from an ombrotrophic peat bog*, Geoderma 135 (2006), pp. 196–203.
[31] A.L.R. Sekaly, R. Mandal, N.M. Hassan, J. Murimboh, C.L. Chakrabarti, M.H. Back, D.C. Grégoire, and W.H. Schroeder, *Effect of metal/fulvic acid mole ratios on the binding of Ni(II), Pb(II), Cu(II), Cd(II), and Al(III) by two well-characterized fulvic acids in aqueous model solutions*, Anal. Chim. Acta 402 (1999), pp. 211–221.
[32] A.K. Pandey, S.D. Pandey, and V. Misra, *Stability constants of metal–humic acid complexes and its role in environmental detoxification*, Ecotox. Environ. Safe. 47 (2000), pp. 195–200.
[33] R. Kautenburger, *Influence of metal concentration and the presence of competing cations on europium and gadolinium speciation with humic acid analysed by CE-ICP-MS*, J. Anal. Atom. Spectrom. 24 (2009), pp. 934–938.
[34] O. Pourret and R.E. Martinez, *Modeling lanthanide series binding sites on humic acid*, J. Colloid Interface Sci. 330 (2009), pp. 45–50.
[35] H.P. Beck, U. Keuth, H. Schank, and H. Wagner, *Characterization and fractionation of humic acid and determination of complex formation constants with toxic heavy metals*, in *Influence of Humic Acids on the Migration Behaviour of Radioactive and Non-Radioactive Substances Under Conditions Close to Nature. Final Report*, C.M. Marquardt, ed., Forschungszentrum Karlsruhe GmbH, Karlsruhe, 2000. pp. 79–124. Available at http://www.ubka.uni-karlsruhe.de/vvv/fzk/6557/6557.pdf.